JOURNAL OF VIROLOGY, Sept. 1980, p. 775-789
0022-538X/80/09-0775/15$02.00/0

Vol. 35, No. 3

Role of the Host Cell in Bacteriophage T4 Development

II. Characterization of Host Mutants That Have Pleiotropic Effects on T4 Growth

BARBARA L. STITT,† HELEN R. REVEL,‡ ILGA LIELAUSIS, AND WILLIAM B. WOOD§*

Division of Biology, California Institute of Technology, Pasadena, California 91125

Mutant host-defective *Escherichia coli* that fail to propagate bacteriophage T4 and have a pleiotropic effect on T4 development have been isolated and characterized. In phage-infected mutant cells, specific early phage proteins are absent or reduced in amount, phage DNA synthesis is depressed by about 50%, specific structural phage proteins, including some tail and collar components, are deficient or missing, and host-cell lysis is delayed and slow. Almost all phage that can overcome the host block carry mutations that map in functionally undefined 'nonessential" regions of the T4 genome, most near gene 39. The mutant host strains are temperature sensitive for growth and show simultaneous reversion of the *ts* phenotype and the inability to propagate $T4^+$. The host mutations are cotransduced with *ilv* (83 min) and may lie in the gene for transcription termination factor rho.

Roles for the *Escherichia coli* host cell in the assembly of bacteriophage T4 have been identified in the processes of phage capsid formation (7, 11, 45), tail fiber assembly (35), and possibly tail assembly (42, 40). We have made an extensive search for host-defective (HD) bacterial mutants that affect the assembly of bacteriophage T4. All mutants that specifically block morphogenesis are found to act during phage capsid formation at the level of T4 gene 31 function (37). One class of HD mutants, designated HDF, shows multiple effects: T4 DNA synthesis is delayed, yet infected cells synthesize significant amounts of phage DNA and eventually lyse without production of infectious progeny, as if the defect were in phage assembly.

In this paper we report investigations into the nature of the HDF host defect. We have examined the phenotypes of $T4^+$-infected and uninfected HDF cells, and we have determined the map positions of the bacterial mutation and the mutations carried by T4 mutant phages that can overcome the host defect. The results support the suggestion (5, 41) that HDF strains, similar strains with mutations at a locus designated *tabC* (5, 43), and another similar strain designated HD590 (41) carry mutational alterations in the gene for the bacterial transcription termination factor rho.

† Present address: Public Health Research Institute of the City of New York, Inc., New York, NY 10016.

‡ Present address: Department of Molecular Biology and Microbiology, Tufts Medical School, Boston, MA 02111.

§ Present address: Department of Molecular, Cellular and Developmental Biology, University of Colorado, Boulder, CO 80309.

(These studies are included in the doctoral dissertation of B.L.S., submitted in partial fulfillment of the requirements for the Ph.D. degree, California Institute of Technology, Pasadena, 1978. A preliminary report of some of the studies described here has been published [52].)

MATERIALS AND METHODS

Materials and methods not reported below have been described previously (37).

Media. Tryptone top and bottom agars contained, per liter, 6.5 and 10 g of agar (Difco Laboratories, Detroit, Mich.), respectively, in addition to 10 g of tryptone (Difco) and 5 g of NaCl.

Chemicals and enzymes. Threefold recrystallized egg white lysozyme, crystalline vitamin B_{12}, L-homocysteine, Tween 40, and DL-α-glycerophosphate were from Sigma Chemical Co., St. Louis, Mo. Oleic acid was from Mallinkrodt; stearate and palmitate were from Serdary Research Laboratories, London, Ontario, Canada.

Radioactive compounds. [2-^{3}H(N)]glycerol (200 mCi/mmol) and 2,6-[1,7-^{14}C]diaminopimelic acid (105 mCi/mmol) were from New England Nuclear Corp., Boston, Mass. [^{14}C]leucine was used at a specific activity of 312 mCi/mmol.

Bacteria and bacteriophages. *E. coli* K-12 strain SKB178, obtained from A. D. Kaiser, was used for the selection of HD mutants. The properties of SKB178 and the HDF strains derived from it are given in Table 1. B011′ *thy sup str* and HD590 *thy sup str hdf* are, respectively, an amber suppressor strain of *E. coli* B and an HDF-type mutant derived from it (42). *E. coli* Bb, nonpermissive for amber mutants, was used for the preparation of extracts for most in vitro complementation experiments. B/5 and S/6/5 are B strains nonpermissive for amber mutants. CR63 is a K-12

TABLE 1. *Properties of HDF strains derived from SKB178*

Bacterium	Markers present	Comments
SKB178	*galE* RglI	Parent of HDF strains
HDF12.5	*galE metG*[a] *hdf* Suc[b] Rgl I	Temperature sensitive at 45°C; at 37°C, 4% "snakes" in H broth, 0% in M9
HDF0.26	*galE glp*[c] *hdf* T6[r] Rgl I	*ts*[+] derivative of original *ts*HDF0.26; 100× normal spontaneous mutation rate
HDF3.41	*galE glp*[c] *hdf* Rgl I	Temperature sensitive at 42°C; adsorbs T4 poorly after growth in M9
HDF3.03	*galE glp*[c] *hdf* Rgl I	Temperature sensitive at 42°C; *hdf* allele is leaky; fails to grow phage P1

[a] The *metG* mutation was identified by (i) the amino acid requirement, (ii) the inability to grow in M9 supplemented with vitamin B_{12} and homocysteine (2), and (iii) map location (covered by plasmid F103).

[b] The Suc phenotype indicates lack of growth on sodium succinate as carbon source; the mutation may affect electron transport (8) and may be in *ubiG*.

[c] HDF0.26, HDF3.03, and HDF3.41 each have a mutation in a *glp* gene, possibly in *glpT* or *glpA*. HDF0.26 and HDF3.03 do not grow on DL-α-glycerophosphate as the carbon source. HDF3.41 fails to incorporate [^{3}H]glycerol into phospholipids (data not shown).

strain permissive for amber mutants; CR63(λ) is nonpermissive for T4 *r*II mutants. CT196 and CT439 are wild nonsuppressing California Institute of Technology (Caltech) "hospital" strains (50), nonpermissive for T4 mutants carrying delections in the gene 39–gene 56 region (15) and the tRNA region (50), respectively.

T4 single and multiple amber mutant strains, listed in Tables 2 and 3, are from the Caltech collection (now maintained in the Department of Molecular, Cellular and Developmental Biology, University of Colorado, Boulder). T4 *go* mutant phages were selected as described previously (37). Lysozyme deletion mutants of T4 (*eG*19, *eG*79, *eG*223, and *eG*298) and tRNA deletion mutants (psu_b-Δ64 and psu_b-Δ33) have been described by Wilson et al. (51). The *r*II deletion strains used are *rEDdf*41 (21) and *r*1589 (1). T4 strains carrying deletions in the nonessential region between genes 39 and 56 [*del*(39–56)1, -3, -4, -5, and -12] were provided by T. Homyk (15). The mutation [*del*(39–56)12] is in a T4D genetic background, whereas the other *del*(39-56) mutations are in T4B. All *del*(39-56) strains carry the *r*II deletion *r*1589.

Genetic crosses. Phage crosses were carried out as described previously (37).

Measurement of phage DNA synthesis. Bacterial cells were grown in H broth to 10^8 per ml and concentrated to 2×10^8 per ml in the same medium. A 10-ml flask containing 2 ml of cells was placed in a shaking water bath at 37°C at $t = -2$ min. At $t = 0$ min, phage were added at a multiplicity of infection of 6 to 8. At $t = 3$, deoxyadenosine at a final concentration of 200 μg/ml and [^{14}C]thymidine at a final concentration of 6 μg/ml and a specific activity of 5 to 10 μCi/μmol were added. At various times 0.1-ml samples were pipetted into 2 ml of ice-cold 5% trichloroacetic acid containing 50 μg of unlabeled thymidine per ml. After 30 min at 0°C, the samples were filtered through Whatman GF/A glass filters; the filters were washed with 4 volumes of 5% trichloroacetic acid containing thymidine and then with 2 volumes of 95% ethanol; they were then dried and counted in 5 ml of toluene-Liquifluor scintillation fluid.

In vitro complementation tests. The presence of active major phage structures (heads, tails, and tail fibers) in T4[+]-infected HDF strains was assayed as described in reference 37. The assays for whole baseplates and tail-baseplate gene products were as described (20), with the following modifications. Cultures (250 ml) of *E. coli* strain Bb were infected (and superinfected at $t = 10$ min in cases where no *t* mutation was present) at multiplicity of infection of 7. HDF-infected cells were aerated for 35 min at 37°C and then chilled for 10 min before harvesting by centrifugation. A 20-μl amount of DNase and 40 to 50 μl of Tris-magnesium (TMg) buffer, pH 7.4 (37), were blended in a Vortex mixer with the infected cell pellets before freezing. The in vitro complementation reaction mixtures consisted of 20 μl of each extract and were incubated at 30°C for 3 h before assay of plaque-forming phage.

TABLE 2. *T4 amber mutants: single*

Gene	Mutation
3	*amNG*131
5	*amN*135
6	*amN*102 *amB*251
7	*amB*16
8	*amN*132
9	*amE*17
10	*amB*255
11	*amN*128
12	*amN*69
15	*amN*133
18	*amE*18
19	*amE*1137
23	*amB*17
25	*amS*52
26	*amS*105
27	*amN*120
28	*amA*452
29	*amB*7
39	*amN*116 *amNG*457 *amE*480
51	*amS*29
53	*amH*28
54	*amH*21
60	*amE*300
e	*amH*26 *tsC*3

TABLE 3. *T4 amber mutants: multiple*

Strain	Defective genes	Mutations
X77	34:34:37	*amB*25:*amA*455:*amN*52
X143	18:27	*amE*18:*amN*120
X379	23:63:*r*II	*amB*17:*amM*69:*rEDdf*41
X381:*t*	5:6:7:*t*	*amB*256:*amB*251:*amB*16:*amB*5
	15:*t*	*amN*133:*amB*5
	19:*t*	*amE*1137:*amB*5
	48:*t*	*amN*85:*amB*5

Tail fiber antigen determination. The endpoint serum blocking assay was used as described previously (49), except that twofold dilutions of the sample were made in the serum and 2,500 tester phage were added.

Assay of bacterial protein synthesis. Cells were grown to 8×10^7 per ml in M9 medium plus all amino acids, thiamine, 10^{-5} M $FeCl_3$, and thymine, concentrated to 4×10^8 per ml in the same medium minus leucine, and diluted 40-fold into the supplemented medium containing 2 μCi of [^{14}C]leucine per ml. Samples, 40 μl, were taken every 15 min and added to 2 ml of ice-cold 10% trichloroacetic acid containing 50 μg of leucine per ml. After at least 30 min, samples were filtered through Whatman GF/A glass filters; the filters were washed with 4 volumes of 5% trichloroacetic acid containing cold leucine followed by 2 volumes of 95% ethanol, dried, and counted in 5 ml of toluene-Liquifluor scintillation fluid.

Assay of bacterial DNA synthesis. Cells were grown to 4×10^8 per ml and diluted 40-fold into prewarmed H broth containing 100 μg of deoxyadenosine and 1 μCi of [^{14}C]thymidine per ml. Samples, 50 μl, were taken at 15-min intervals into 2 ml of ice-cold 10% trichloroacetic acid and prepared for counting as above.

Assay of bacterial cell wall synthesis. Cells were grown to 4×10^8 per ml and diluted 40-fold into prewarmed M9 containing 0.05% Casamino Acids, thiamine, 10^{-5} M $FeCl_3$, and 3 μCi of [^{14}C]diaminopimelic acid per ml. Samples (50 μl) were taken at 15-min intervals into 2 ml of ice-cold 10% trichloroacetic acid and prepared for counting as above.

Assay of bacterial phospholipid synthesis. The procedure for assay of bacterial phospholipid synthesis is a modification of methods described by Mindich et al. (31), Goldfine (12), and Radin (36). Cells were grown to 8×10^7 per ml in M9 plus 0.05% Casamino Acids, thiamine, 10^{-5} M $FeCl_3$, and 20 μg of glycerol per ml, concentrated to 4×10^8 per ml, and diluted 40-fold into fresh prewarmed medium containing 25 μCi of [^{3}H]glycerol per ml. Samples (20 μl) were taken in duplicate every 15 min, applied to Whatman GF/C glass fiber filters, and plunged into 5 ml of ice-cold 10% trichloroacetic acid, which was decanted after 30 min and replaced by 5% trichloroacetic acid for 15 min and then by two 30-min rinses of cold water. One set of samples was then dried and counted; the second was rinsed three times with 3 ml of 2:1 chloroform-methanol before drying and counting. Incorporation of glycerol into phospholipid was determined by subtracting the radioactivity in the chloroform-methanol-extracted samples from that in the unextracted samples.

RESULTS

Isolation and initial characterization of HDF strains. Several hundred HD bacteria that absorb T4 but are unable to support its growth were isolated from *E. coli* K-12 strain SKB178 after nitrosoguanidine mutagenesis and selection of surviving colonies that grow in the presence of T4 and T6 (37). The bacterial HD mutant strains were grouped into seven classes by the plating properties of four spontaneous T4 mutants carrying compensating mutations (*goA*1, *goC*1, *goD*1, and *goF*1), selected by plating high concentrations of T4$^+$ on a limited set of HD strains. HDF strains are able to propagate only the *goF*1 mutant phage. Additional HDF strains were obtained after nitrosoguanidine mutagenesis and selection in the presence of *goA*1 and T6 (37). The latter procedure increased the frequency of HDF strains from 2 to 25% of total HD mutants. Most experiments were repeated on several independent HDF mutants with similar results; data presented here are chiefly for HDF12.5.

The efficiencies of plating of T4$^+$ and the burst sizes of T4$^+$ and *goF*1 on HDF strains are given in Table 4. Although the effectiveness of the host block appears to vary widely as measured by efficiency of plating, the burst size measurements show that phage production is virtually eliminated in T4$^+$-infected HDF cells at 37°C in liquid medium. The *goF*1 mutation restores phage burst size to 20 to 25% of the normal level. In these experiments phage absorption to and

TABLE 4. *Plating properties and burst sizes of T4$^+$ and goF phages on various hosts*

Bacterial strain	T4$^+$			*goF*1		*goF*3.03-2	
	BS,[a] 25°C	BS, 37°C	EOP,[b] 37°C	BS, 37°C	Spot,[c] 37°C	BS, 37°C	Spot, 37°C
SKB178	60	150	1.0	120	+	90	+
HDF12.5	42	0.5	10^{-6}	32	+	0.3	−
HDF0.26	60	0.5	10^{-5}	30	+	1.0	−
HDF3.41	17	0.1	10^{-4}	3	+	0.03	−
HDF3.03	56	1.0	10^{-2}	15	+	5.0	+
B011	70	200	1.0	90	+	NT[d]	+
*hd*590	12	0.01	10^{-6}	20	+	NT	−

[a] BS, Burst size; all measurements are averages of two or more determinations.

[b] EOP, Efficiency of plating relative to SKB178.

[c] Spot test for growth: + indicates that approximately the same number of plaques were found on the strain in question as on wild-type cells when 10 μl of phage at 10^4 per ml was spotted on a seeded plate; − indicates that no plaques were found and the EOP is $<10^{-2}$.

[d] NT, Not tested.

killing of HDF mutant hosts was normal (data not shown). The temperature dependence of the ability of HDF strains to support T4 growth is also shown in Table 4. At 25°C the burst size of $T4^+$ in HDF bacteria is almost normal.

Upon initial isolation all HDF strains were temperature sensitive for bacterial growth: bacterial lawns at 42°C were either very sparse or nonexistent on EHA, LB, or tryptone plates. Cell growth did not stop immediately in liquid culture at 42°C; during a 2-h observation period the cell doubling time increased from 30 min at 37°C to 50 to 80 min at the restrictive temperature. The original temperature-sensitive strain of HDF0.26 was lost; all experiments with HDF0.26 have been done with a spontaneous ts^+ derivative of the original.

The ability of some other phages to grow on HDF mutant hosts was determined by spot test. Phages T2 and T6 behave like T4, whereas lambda, T3, T5, T7, and P1 grow on all HDF strains, with the single exception that P1 fails to grow on HDF3.03.

Course of infection in $T4^+$-infected HDF strains. (i) Phage DNA synthesis is delayed and depressed. DNA synthesis after phage infection was measured by the continuous incorporation of [^{14}C]thymidine into acid-insoluble material (Fig. 1). The results show that the rate of $T4^+$ DNA synthesis in HDF12.5 is about half that in the parental host and that there is a 3- to 6-min delay in the initiation of DNA synthesis. In *goF*1 infection of HDF12.5, the rate of DNA synthesis is increased, but the delay is still present, suggesting that factors affecting the rate of DNA synthesis are more crucial to phage production than those affecting time of initiation. DNA synthesis in SKB178 infected with *goF*1 is normal.

(ii) Assembly of phage structures is defective or absent. Table 5 shows that no active heads, tails, or free baseplates could be demonstrated in extracts of $T4^+$-infected HDF cells by in vitro complementation tests. The subnormal level of active tail fibers observed in these experiments was verified by serological measurements of tail fiber antigens in the same extracts (data not shown). The absence of active major structural assembly intermediates was confirmed by electron microscopy of negatively stained lysates of phage-infected cells. Whereas control lysates of $T4^+$-infected wild-type cells showed the expected filled heads, tails, and free baseplates, lysates of $T4^+$-infected HDF cells showed chiefly empty heads and rare polyheads and polysheaths, but no tails or baseplate structures (data not shown).

The presence of polysheath, the product of aberrant polymerization of gp18 that appears late in normal infection and earlier in the absence of baseplate production (22), suggested that in $T4^+$-infected HDF cells some tail proteins might be present but unable to assemble normally because of a defect in baseplate morphogenesis. Further in vitro complementation analysis of all tail gene products revealed that the core and sheath components gp3, gp15, gp18, and gp19 from $T4^+$-infected HDF cells are active (Table 6). Among the baseplate components, however, only gp9 and gp12 show significant in vitro activity. These results suggest that the abortive baseplate assembly is due to decreased levels of many proteins rather than a block at a specific assembly step. Impaired synthesis or increased degradation of baseplate proteins could account for these observations, in view of the finding that in vitro baseplate complemen-

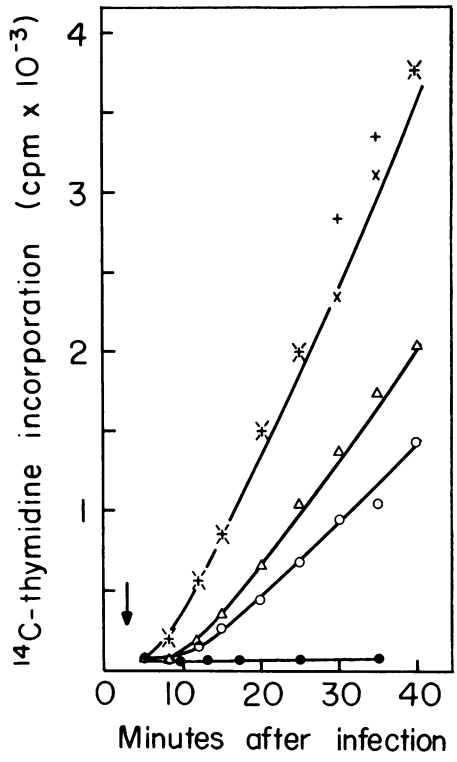

FIG. 1. *Incorporation of [^{14}C]thymidine in five T4-infected cell cultures as a measure of phage DNA synthesis. The arrow indicates the time of addition of [^{14}C]thymidine, after which samples were taken at various times and trichloroacetic acid-precipitable radioactivity was determined. Symbols: +, SKB178 infected with $T4^+$; ×, SKB178 infected with goF1; Δ, HDF12.5 infected with goF1; ○, HDF12.5 infected with $T4^+$; ●, SKB178 infected with the gene 42 mutant am122 (DNA-negative phenotype). The am122 experiment shows that the observed thymidine incorporation is a measure of phage DNA synthesis. For details of the procedure see text.*

TABLE 5. *In vitro complementation of T4⁺-infected HDF extracts with defective extracts supplying major phage structures*[a]

Complementing extract	Plaque-forming phage × 10^{-9}					
	Head defective	Tail and baseplate defective	Baseplate defective	Tail defective	Tail fiber defective	T4⁺ + HDF12.5
T4⁺ + HDF12.5	9.3	11.6	11.0	—[b]	62	7.9
Tail fiber defective	480	200	—	—	3.2	
Tail defective	—	—	470	3.6		
Baseplate defective	—	—	0.5			
Tail and baseplate defective	60	0.4				
Head defective	1.3					

[a] Fifty microliters each of two extracts were mixed, incubated for 3 h at 30°C, and then assayed for plaque-forming phage. Results are expressed as plaque-forming phage per milliliter of reaction mixture. Extracts were prepared as described in Revel et al. (37). The head-defective preparation (tail and tail fiber donor) was an extract made from SKB178 infected with *amB*17 (gene 23 defective); the tail- and baseplate-defective preparation (head and tail fiber donor) was an extract made from SKB178 infected with X143 (genes 18:27 defective); the baseplate-defective preparation (head and tail fiber donor) was an extract made from Bb infected with X381:*t* (genes 5:6:7:*t* defective); the tail-defective preparation (head, baseplate, and tail fiber donor) was an extract made from Bb infected with *amE*1137:*amB*5 (genes 19:*t*-defective); and the tail fiber-defective preparation (donor of particles lacking tail fibers) was an extract made from SKB178 infected with X77 (genes 34:34: 37-defective).

[b] —, Not tested.

TABLE 6. *In vitro complementation assays for the presence of tail proteins in extracts of T4⁺-infected HDF*[a]

Tail structure missing from test extract	Mutant gene	Plaque-forming phage × 10^{-9}		
		Uncomplemented controls	Baseplate defective	T4⁺ + HDF
Sheath	18	0.1	220	30
Tube	19	3.8	670	370
Connector	3	32	1000	91
	15	6.8	600	350
Baseplate plug	29	2.1	86	3.0
	26	1.8	20	2.0
	28	2.6	194	3.0
	51	2.6	10	3.0
	5	0.4	130	2.2
	27	1.0	60	2.7
Baseplate wedge	10	0.1	67	1.7
	11	75	65	42
	7	1.0	130	2.1
	8	1.3	52	8.0
	6	8.0	280	10.0
	53	0.6	46	1.6
	25	5.4	28	2.6
Baseplate completion proteins	48	2.7	74	7.7
	54	0.2	31	0.8
	9	5.6	450	310
	12	3.7	290	80

[a] Twenty microliters each of two extracts were mixed, incubated for 3 h at 30°C, and then assayed for plaque-forming phage. Results are expressed as plaque-forming phage per milliliter of reaction mixture. Extracts were prepared as described in the text. The baseplate-defective control extract was made from strain Bb infected with a baseplate structural gene mutant (gene 5, 7, or 8; different from the mutant gene in the test extract). The T4⁺ + HDF extract was made from HDF12.5 infected with T4⁺.

tation reactions are extremely concentration dependent (20).

(iii) Patterns of phage-induced protein synthesis are altered. Electrophoretic analysis of proteins synthesized after phage infection shows that a few specific early and late proteins are decreased in amount or absent in T4⁺-infected HDF cells (Fig. 2). Specifically, gp43 and four early or middle proteins of molecular weights about 58,000, 43,000, 36,000, and 26,000 are reduced in T4⁺-infected mutant hosts. The identity of the latter four proteins is unknown, although electrophoretic analysis and in vitro complementation tests have shown that the 43,000-dalton protein is not gp63 and that the 58,000-dalton protein is neither gp39 nor gp30, but may be gp41 or an unknown protein that migrates with it in electrophoresis (data not shown). The unidentified early proteins of 43,000 and 36,000 daltons are missing at late times in the T4⁺-infected HDF cells under both nonpermissive (37°C) and permissive (25°C) conditions (Fig. 3).

At least four viral structural proteins normally synthesized late in infection, gp34, gp7, gp37, and gp*wac* are clearly reduced in T4⁺-infected HDF cells under nonpermissive conditions. These structural proteins are made at normal levels under conditions permissive for phage growth, that is, in *goF*1 infection of HDF0.26 at 37°C and T4⁺ infection of HDF0.26 at 25°C (Fig. 3). Many of the baseplate proteins migrate to crowded regions of the gel, so that assessment of their presence or absence is difficult.

Finally, some proteins are overproduced in the abortive T4⁺ infection of HDF cells: bands

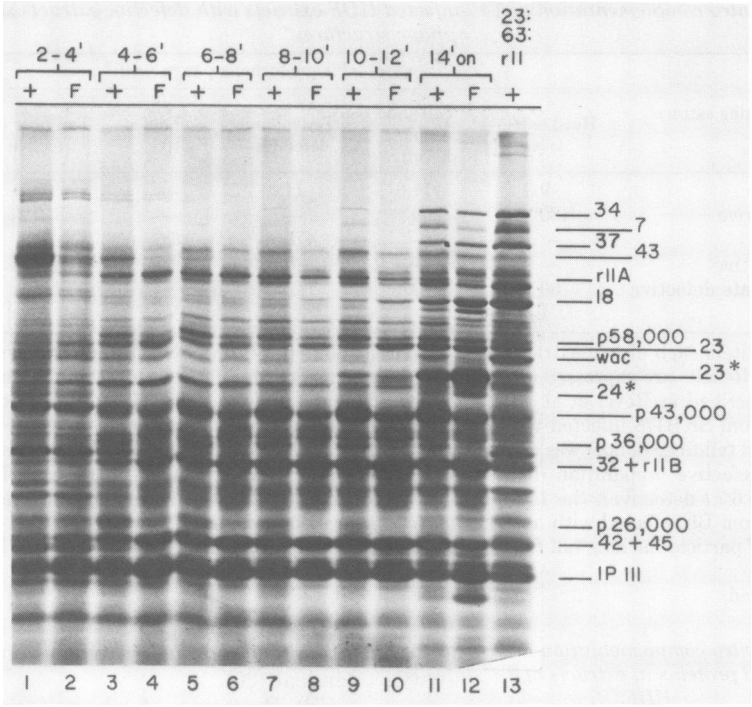

FIG. 2. *Time of appearance of phage proteins in T4⁺-infected HDF0.26. HDF0.26 was used for most protein labeling experiments in place of HDF12.5, which behaves anomalously under the conditions used for labeling (see text). Cultures prepared as described in the text were labeled for the indicated periods, chased, and prepared for electrophoresis on a 10% polyacrylamide gel as described by Revel et al. (37). "+" indicates T4⁺ infection of SKB178; "F" indicates T4⁺ infection of HDF0.26. Bands are labeled as the products of T4 genes where known, or by a "p" followed by their estimated molecular weight. At early times numerous bacterial bands are visible, particularly in the 2- to 4-min labeling period. Most phage bands were identified by the comparison of proteins made in wild-type infections with those made in infections of nonpermissive cells with phage containing known amber mutations. The identifications of gp7, gp43, pg32, and gp22 were made by comparison with published electropherograms (33, 48). Molecular weights of unidentified bands were estimated from a plot of migration distances of known bands through a 10% gel against the logarithms of their molecular weights. Such plots were found to be linear from approximately 80,000 to at least 20,000 daltons. 23:63:rII indicates infection of SKB178 with a phage carrying the mutations amB17, amM69, and rEDdf41.*

on electrophoresis gels corresponding to gp32 + *r*IIB and to gpIPIII are more intense than normal in analyses of samples taken throughout infection, and a band just below gp23* appears more intense than normal in samples taken late in infection (Fig. 3). Overproduction of gp32, the DNA binding protein, could be a result of aberrant DNA synthesis (25).

(iv) Cell lysis is delayed. Although T4⁺-infected HDF strains do not produce active progeny phage, the infected cells do undergo lysis. However, lysis of T4⁺-infected HDF12.5 is delayed about 20 min compared with lysis of T4⁺-infected SKB178, and cell distintegration during lysis proceeds more slowly (Fig. 4). When shaken with chloroform, both T4⁺-infected HDF cells and wild-type cells lyse promptly at times subsequent to 12 to 15 min postinfection at 37°C (data not shown). This result suggests that in T4⁺-infected HDF cells lysozyme production is close to normal, but retarded breakdown of the bacterial inner membrane limits access to the cell wall, thus delaying the lysis process. In *goF*1 infection of HDF strains the delay in lysis is reduced but still evident (data not shown). This observation is consistent with burst size measurements, which indicate that the *goF*1 mutation does not fully compensate for the host defect (see Table 4).

(v) The host component defined by *hdf* mutations is required throughout T4 infection. T4⁺ growth in HDF cells is strongly influenced by the temperature during phage infection (Table 4) but is independent of the temperature at which cells are cultivated before infection. Cells that are grown at 37°C, poisoned with KCN, shifted to 25°C, infected with T4⁺, and then diluted to relieve KCN inhibition produce

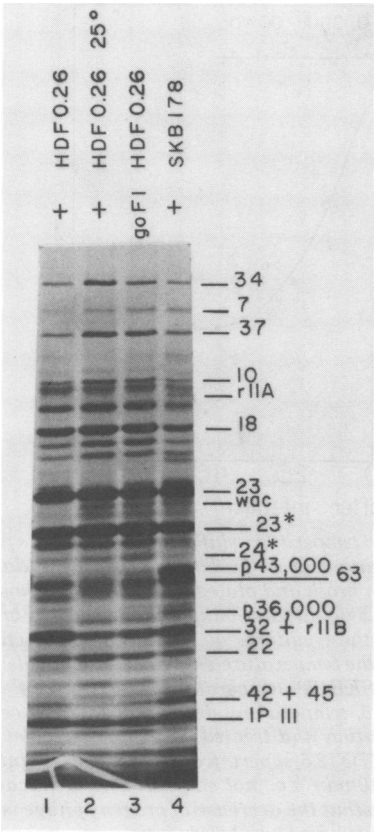

FIG. 3. *Gel electrophoresis of T4 proteins synthesized in HDF0.26 under permissive and nonpermissive conditions. The phage and host used for sample preparation are indicated immediately above each track; + indicates T4⁺. All infections were at 37°C unless otherwise indicated. Cells labeled at 37°C received 1 μCi of ^{14}C-amino acids at 20 and 25 min after infection (the label was chased with unlabeled amino acids at 30 min), and those labeled at 25°C received 1 μCi at 45 and 57 min after infection (the label was chased with unlabeled amino acids at 70 min). The gel is a 12-cm, 30-ml exponential gradient at 7.5 to 20% acrylamide poured by holding the volume of acrylamide in the mixing chamber constant at 5.0 ml.*

the same normal phage burst as cells grown at 25°C (data not shown). In analogous shift-up experiments, in which cells were cultivated at 25°C and then shifted to 37°C at the time of infection, phage growth was inhibited just as in HDF cells grown continuously at 37°C. These results suggest that the activity of the temperature-sensitive component in HDF cells is reversibly temperature labile.

Because of this feature, temperature shifts performed after phage adsorption can be used to determine the period during the infection cycle when the host component is required for T4 growth. Shift-up of T4⁺-infected HDF cells from 25 to 37°C at any time after appearance of the first progeny phage leads to immediate cessation of phage production, as indicated by the congruence of the intracellular phage growth curve and the curve for phage produced by 140 min after infection (Fig. 5a). This result suggests that the labile host function is essential for phage production throughout the latter part of the infectious cycle and that it is inactivated immediately after a shift to high temperature.

Shift-down experiments (Fig. 5b) show that the longer T4⁺-infected HDF cells are held at 37°C before shift, the smaller the burst size. Since burst size reduction is evident after shifts as early as 5 min after infection at 37°C, the host function is clearly needed at early times, perhaps even before phage DNA synthesis starts (see Fig. 1). Considered together, the temperature shift experiments show that the host component is essential throughout the phage infection cycle.

T4 *goF* mutants compensate for the HDF host defect. The T4 mutant *goF*1, used to identify class F HD bacteria, grows normally in wild-type bacteria and by definition grows on all HDF strains. However, its burst size is only about 25% of normal on HDF strains, indicating that compensation is incomplete (Table 4). The *goF*1 mutant site was initially located in the gene 39 region by a series of crosses of *goF*1 with phage carrying multiple amber mutations situated around the genome. Its location clockwise from gene 39 was established by two- and three-factor crosses with gene 60 and gene 39 amber mutations, using an *r*II deletion as an outside

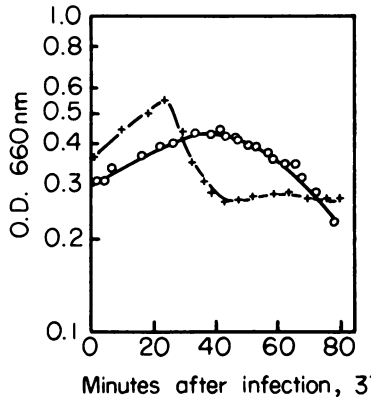

FIG. 4. *Lysis of HDF12.5 cells after phage infection. Cells at 2 × 10⁸ per ml in H broth were infected at a multiplicity of infection of 5, and samples were taken at the times shown for determination of optical density (O.D.) at 660 nm. Symbols: +, SKB178 infected with X77; ○, HDF12.5 infected with X77. X77 was used instead of T4⁺ to avoid the possibility of lysis inhibition by superinfecting progeny phage.*

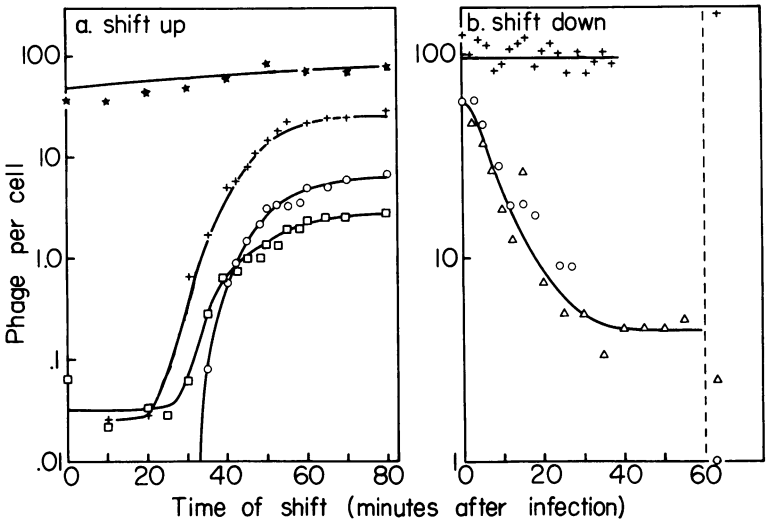

FIG. 5. *Phage production in infected-cell cultures subjected to temperature shifts. (a) Infected cells prepared as described in the legend to Fig. 4 were incubated with aeration at 27°C. To follow intracellular phage growth, samples were diluted at 2-min intervals into chloroform broth and plated on a permissive host. Other samples were shifted from 27 to 37°C at the indicated times by 200-fold dilution into prewarmed H broth and aerated at the higher temperature. Chloroform was added to these cultures at 140 min after infection, and samples were plated on CR63 to assay total phage produced in the temperature-shifted cells. Symbols: +, T4⁺-infected SKB178, intracellular growth curve; *, T4⁺-infected SKB178, temperature shifted; ○, T4⁺-infected HDF12.5, intracellular growth curve; □, T4⁺-infected HDF12.5, temperature shifted. (b) Infected cells were shifted form 37 to 25°C at the indicated times by 200-fold dilution and treated as in (a). Symbols: +, T4⁺-infected SKB178; ○, T4⁺-infected HDF12.5; △, T4⁺-infected HDF12.5 superinfected with T4⁺. Points to the right of the dashed line are from samples kept at 37°C for 140 min (i.e., not shifted). The identical results obtained for superinfected and nonsuperinfected HDF12.5 show that the decrease in progeny phage is not due to a decrease in the amount of time available at the permissive temperature before lysis.*

marker. Finally, by crosses of *goF*1 with various phages carrying deletions in the gene 39–56 region, the mutant site was placed between the left ends of *del*(39–56)5 and *del*(39–56)3 (Fig. 6) in a nonessential region of the genome. The *goF*1 mutation is not in gene 39, based on the following observations. The deletion mutant *del*(39–56)12 fails to yield wild-type recombinants when crossed with *goF*1 and therefore must lack at least part of the gene in which the *goF*1 mutation lies. However, *del*(39–56)12 forms plaques under conditions that require gene 39 function and makes a product identifiable on sodium dodecyl sulfate-acrylamide gels as gp39 (Fig. 7).

Further experiments with deletion mutants indicate that the *goF* phenotype depends upon functional alteration of a phage gene product rather than its elimination. The *del* (39–56)12 mutant, which apparently lacks the *goF*1⁺ site, grows in wild-type hosts but fails to grow in HDF hosts. In contrast, the multiple mutants *goF*1:*del*(39–56)3 and *goF*1:*del*(39–56)4, which carry only slightly smaller deletions than *del*(39–56)12 (15), do grow in HDF strains.

The results of mixed infections of HDF12.5 with wild-type (*goF*⁺) phage and phage carrying the *goF*1 mutation are shown in Table 7, experiments 1 to 6. The observed burst sizes are intermediate between those for HDF12.5 infected with *goF*⁺ alone and *goF*1 alone. Similar results are found in mixed infections with *goF*1 and *del*(39–56)12, which lacks the *goF* locus (Table 7, experiments 7 to 12). These findings suggest that the *goF*1 allele is dominant in mixed infections, but that there may be a dosage dependence of burst size on *goF*1. The skewed output ratio of progeny genotypes obtained in mixedly infected HDF12.5 cells is unexplained.

Although 8 of 13 independently selected *goF* phage mutants resemble *goF*1, the following five are different. (i) *goF*3.03-2 grows only on HDF3.03 and carries a mutation that maps near the T4 lysozyme gene *e* (Table 4, Fig. 8). Because the lysis function of T4 lysozyme apparently is unaffected in wild-type cells infected with *goF*3.03-2 (data not shown), this mutation probably is not in gene *e*. (ii) *goF*3.03-8 carries a mutation that maps in a similar location. This mutant fails to grow on HD590, but unlike *goF*3.03-2, it plates on all K-12 HDF strains. (iii) *goF*0.26-6 also compensates for all HDF defects.

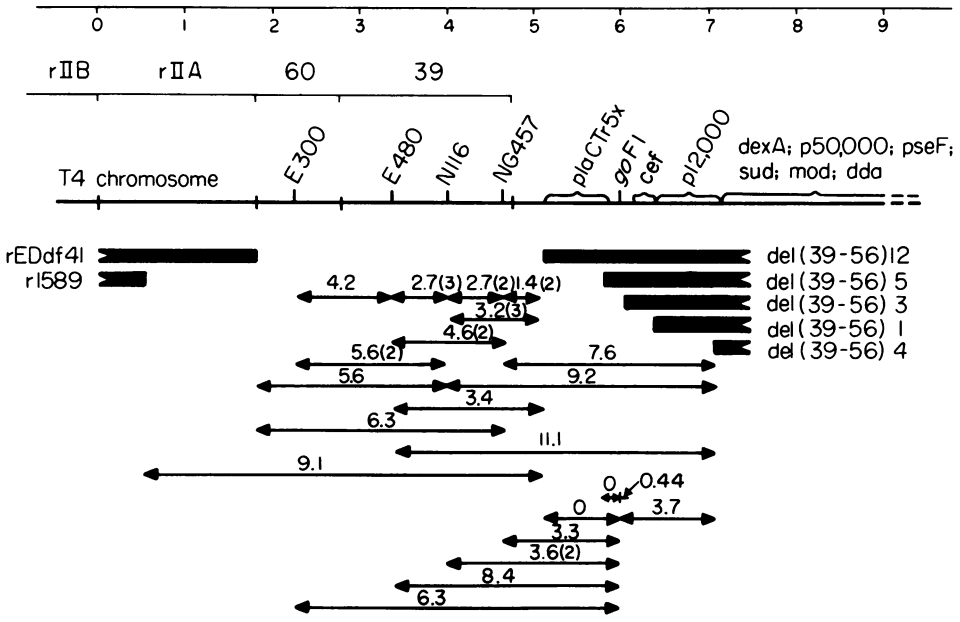

FIG. 6. *Location of goF1 on the T4 genome. The figure shows the positions of point mutations (short vertical lines above the line representing the T4 chromosome) and deletions (heavy bars). The precentages of recombination are shown below; arrows indicate the intervals over which recombination was measured. Numbers in parentheses indicate the number of crosses. A notch at the end of a heavy bar indicates that the deletion continues in that direction. The ends of genes are indicated by vertical lines drawn all the way through the line representing the T4 chromosome. The positions of genes are indicated by labeled brackets. Amber mutations are indicated by number only, without the prefix am. The scale (top line) is measured in kilobase pairs (kb) from an arbitrary zero point at the boundary between rIIA and rIIB (53). The size of the rIIA region, and hence the right endpoint of rEDdf41 (10), is based on the data of Bujard et al. (4) and Kim and Davidson (21). By measuring the distance from del(39–56)1 (previously designated D_J) to rII deletions defining the right ends of rIIA (4,600 base pairs) and rIIB (6,400 base pairs), Bujard et al. (4) estimated the length of the rIIA region to be 1,800 ± 70 base pairs. The right-hand end of r1589 has been placed at 0.5 kb on the basis of data of Homyk and Weil (15), who measured the distance between del(39–56)1 and r1589 to be 5,900 base pairs. The left endpoints of the del(39–56) mutants are defined by the data of Homyk and Weil (15). The size of gene 60 has been estimated from extensive intracistronic mapping (32). The size of gene 39 has been estimated from the polypeptide molecular weight of 64,000 (33). The positions of plaCTr5x and cef are given in reference 15. The crosses were carried out in CR63 at 30°C as described by Revel et al. (37). Total progeny was determined by plating on CR63 at 37°C. Scoring of recombinants and determination of recombination frequency (%R) was as follows: (i) In crosses between amber mutants in the DNA delay genes 39 and 60, wild-type (WT) progeny were determined by plating on S/6/5 at 25°C (32); %R = WT × 200/total progeny. When one of the parental phage also carried a deletion in the rII genes (rEDdf41), the order of the amber mutations with respect to rII was determined by stabbing wild-type progeny from S/6/5 to a lawn of CR63(λ) to distinguish rII^+ from rII^-. (ii) The intervals between rEDdf41 and ambers in gene 39 were determined by crossing rEDdf41:am double mutants with wild-type phage. am^+ phage were determined by plating on S/6/5 at 25°C (= one-half total progeny), and individual plaques were stabbed to lawns of CR63(λ) to distinguish parental am^+:rII^+ from recombinant am^+:rII phage. %R = am^+:rII × 100/number of plaques picked from S/6/5. (iii) The intervals between various del(39–56) deletions and amber mutants in gene 39 were determined by crossing the single mutants. am^+:del^+ recombinants were measured as large plaques on S/6/5 at 25°C. %R = am^+del^+ × 200/total progeny. (iv) The intervals between goF1 and amber mutants in genes 39 and 60 were determined by crossing the single mutants. am^+ phage were determined by plating on S/6/5 at 25°C (= one-half total progeny), and individual plaques were stabbed to lawns of HDF12.5 at 37°C to distinguish parental am^+:$goF1^+$ from recombinant am^+:goF^+. %R = am^+ goF^+ × 100/number of plaques picked from S/6/5. (v) The intervals between goF1 and the (39–56) deletions were determined by crossing the single mutants. Total progeny were determined by plating on CR63, and individual plaques were stabbed to lawns of CT196 (30°C) and HDF12.5 (37°C) to identify the two recombinant type phages. %R = recombinants × 100/number of plaques picked from CR63. (vi) The interval between del(39–56)12 and rII deletion r1589 was determined in a cross between goF1 and del(39–56)12, which also carries r1589. Total progeny were determined by plating on CR63, and individual plaques were stabbed to lawns of CR63(λ) and HDF12.5 to identify rII^+: del(39–56)12 and rII:goF1 recombinants. %R = recombinants × 100/number of plaques picked from CR63.*

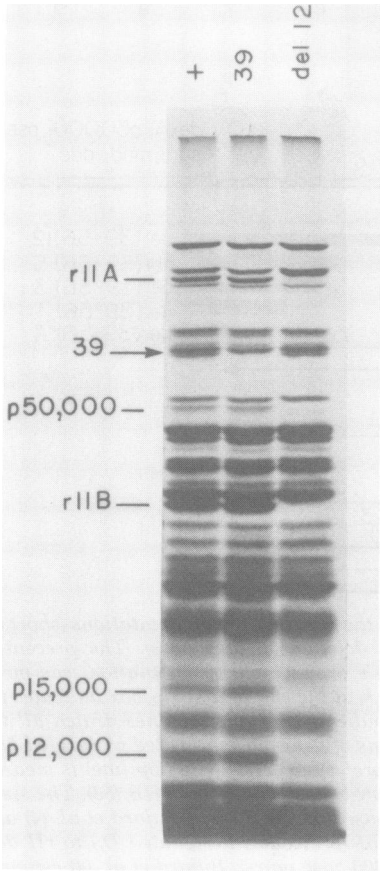

FIG. 7. *Production of gp39 in del(39–56)12:r1589-infected cells. Phage strains used are indicated above each track of the gel; the host was B/5. Bands are identified as described in the legend to Fig. 3. Bacteria grown in M9 at 37°C to 10^8 cells per ml were placed in the bottom of a 150-mm petri dish and gently agitated while being exposed to UV light. The petri dish was placed 36 cm from a germicidal lamp (previously calibrated with phage T4 to give five lethal hits per minute per phage at this distance), and the cells were irradiated for 6 min to reduce host transcription and translation. The cells were then incubated in a 30°C shaking water bath for 10 min before infection. ^{14}C-amino acid-labeled extracts for gel electrophoresis were prepared essentially as described in Revel et al. (37) except for the following: cells were infected at 30°C at a multiplicity of infection of 6 and labeled from 4 to 10 min. At 10 min, 1.5-ml portions of ice-cold 3% Casamino Acids were added to the 2-ml cultures and the cultures were immediately centrifuged. The acrylamide concentration in the separating gel is 10%. gp39, defined by the band missing (arrow) in the amN116(39$^-$) infection, is present in cells infected by either T4$^+$ or del(39–56)12:41589. Other bands missing in del(39-56)12:r1589-infected cells are also indicated. Similar results were observed in SKB178.*

It carries a mutation that has been mapped tentatively to the region between genes 31 and 33. (iv) *goF*0.26-1 plates only on HDF0.26 and HDF12.5; it carries a mutation that maps between genes 55 and *e*. (v) *goF*12.5-3 carries a mutation that maps close to gene 39 but may be a different site than *goF*1, because it makes small plaques on HDF strains 12.5 and 0.26 and fails to grow on HD590.

All *goF* phages grow on the wild-type parental bacterium as well as on all T4$^+$-permissive Caltech hospital strains (50), many of which are nonpermissive for T4 carrying deletions of phage genes that are nonessential in standard laboratory hosts (29).

Location of *hdf* on the *E. coli* chromosome. Genetic mapping of the *hdf* mutation has yielded conflicting results. Using P1 transduction, Simon et al. (41) determined that *hdf* lies near *ilv* at 83 min on the *E. coli* map. We have confirmed this result, showing that *hdf* lies between *ilv* (83 min) and *metE* (84 min). However, in other experiments using the Hfr rapid mapping technique of Low (28), we have obtained evidence of two locations for *hdf*, one at 48 min and the other at 83 min. The 48-min location is confirmed by experiments in which wild-type DNA is introduced into HDF strains via F′ plasmids or lambda transducing phages, but this location is not supported by P1 transduction. The P1-mediated transduction of *hdf* into other K-12 strains is the strongest evidence for its map location, which we therefore believe to be near 83 min. Details and discussion of these observations will be published elsewhere (B. L. Stitt, manuscript in preparation).

Cause of the *ts* phenotype in HDF mutants of *E. coli*. The cotransduction of *hdf* and *ts* markers and the simultaneous reversion of HDF and *ts* phenotypes at frequencies of 10 to 25% (data not shown) in selections for *ts*$^+$ suggest that both phenotypes are caused by the same mutation. In attempts to learn the basis for the *ts* phenotype of HDF strains, we compared the incorporation of several macromolecular precursors before and after a temperature shift from 37 to 42°C in HDF and wild-type cells. No differences were found in the continuous incorporation of [^{14}C]thymidine into DNA, [^{14}C]leucine into protein, or [^{14}C]diaminopimelic acid into cell wall. A 10-fold difference was seen between the abilities of wild-type and some HDF strains to incorporate [^{3}H]glycerol into phospholipids. However, not all HDF strains showed this behavior; furthermore, a derivative of HDF341 made *ts*$^+$ *hdf*$^+$ by transduction with λ*dnaA* (which carries 48-min *E. coli* DNA [24]) phage continued to incorporate glycerol at the lower

TABLE 7. *Dominance relationships of goF⁺ and goF1 alleles*[a]

Expt	Infecting phage(s)	Host	Burst size	% Alleles among progeny	
				goF⁺	*goF*1
1	++(*goF*⁺)	SKB178	148	100	0
2	++(*goF*⁺)	HDF12.5	0.07	100	0
3	*goF*1	SKB178	197	0	100
4	*goF*1	HDF12.5	12.3	0	100
5	++ and *goF*1	SKB178	140	47	53
6	++ and *goF*1	HDF12.5	0.8	25	75
				del(39-56)12	
7	*del*(39-56)12:*r*1589	SKB178	65	100	0
8	*del*(39-56)12:*r*1589	HDF12.5	0.02	100	0
9	*goF*1:*r*1589	SKB178	145	0	100
10	*goF*1:*r*1589	HDF12.5	19.6	0	100
11	*del*(39-56)12:*r*1589 and *goF*1:*r*1589	SKB178	92.5	47	53
12	*del*(39-56)12:*r*1589 and *goF*1:*r*1589	HDF12.5	1.9	20	80

[a] The procedure used for these experiments was the same as that for phage crosses except that the multiplicity of infection of each parental phage was 5. *goF*1:*r*1589 was used in lines 9 to 12 instead of *goF*1 because *del*(39-56)12 also contains the *r*1589 deletion. The genotypes of progeny phage were determined by stabbing 100 plaques per cross from CR63 to lawns of appropriate permissive and nonpermissive bacteria.

level. We therefore conclude that the poor glycerol incorporation is due to a nitrosoguanidine-induced mutation unrelated to *hdf* (see Table 1). We also tried with no success to render HDF cells phenotypically *ts*⁺ by addition of the fatty acid palmitate, stearate, or oleate to either liquid medium or top agar (final concentration of fatty acid, 0.01 to 0.1%, solubilized by 0.01 to 0.1% Tween 40). HDF strains are insensitive to 10 mg of sodium dodecyl sulfate per ml in the growth medium, a crude indication that the cell surface is normal (23). Therefore, the cause of the temperature sensitivity of HDF strains remains unknown.

Comparison of HD590 and HDF strains. The *E. coli* B mutant HD590, isolated and characterized by Simon et al. (42), is phenotypically almost identical to HDF strains, although its block to T4 growth is more stringent. In addition to its effects on T4 DNA and protein synthesis and on phage assembly (42), we found that HD590, like HDF strains, is temperature sensitive for cell growth at 42°C, shows delayed lysis after T4⁺ infection, and is partially permissive for T4⁺ growth at 25°C. Spot tests of T4⁺ at 25°C are negative, but burst size measurements in broth at 25°C give 5 to 25 phage per cell. We find HD590 able to grow in M9 plus thymine but, like HDF12.5, it produces an anomalous pattern of phage proteins under these conditions; that is, proteins known to be present either on the basis of structures seen by electron microscopy or on the basis of in vitro complementation experiments are scarcely detectable on gels. When cells are grown in a richer medium (M9 plus purines, pyrimidines, vitamins, iron, and amino acids except leucine), infected, and labeled with [^{3}H]leucine, both HD590 and HDF12.5 show a pattern of reduced or missing late phage proteins similar to that found with HDF0.26. This pattern differs from that published by Simon et al. (42).

Among 41 *go* phages selected on HD590, 39 were like *goF*1, but 2 were similar to *go*590-1, which carries a mutation in T4 gene 31. The only known function of gene 31 product is in the early stages of T4 head assembly. The *go*590-1-type phage grow in HD590 and in wild-type cells, but not in K-12 HDF strains or in T4 head assembly-defective strains such as HDAD1.1, HDA17.5, *groEA*44 HDD3.6, and *groEA*44, which can be compensated by other mutations in gene 31 (33). Because capsid-like structures are made in T4⁺-infected HD590, the known gene 31 function in head assembly is probably normal. These results suggest that gp31 may have a dual role in T4 development, perhaps required only in *E. coli* B hosts.

DISCUSSION

Summary of the HDF phenotype. The HDF phenotype is complex. Mutant cells absorb T4⁺ normally and are killed by the phage. However, in the subsequent infection some early proteins are underproduced whereas others are overproduced; phage DNA synthesis is depressed; phage capsids are either not filled with DNA or if filled are abnormally unstable; specific late phage proteins are underproduced; and lysis of the infected cell is delayed in onset and slower than normal, although phage lysozyme is present. The host defect responsible for this complex

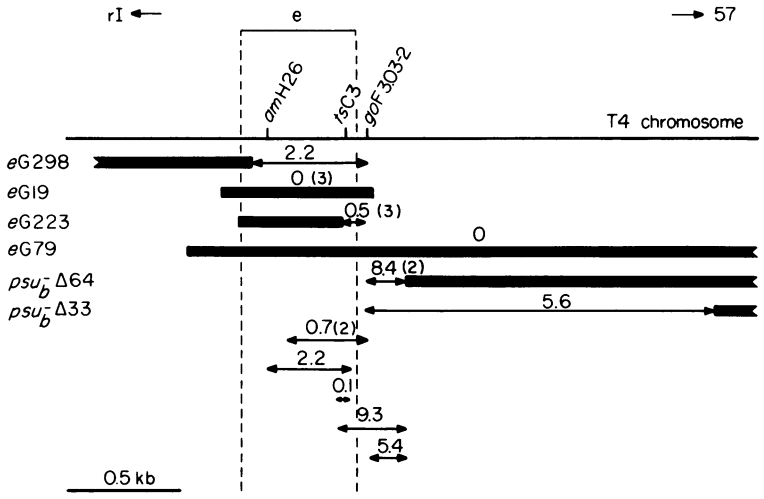

FIG. 8. *Location of goF3.03-2 on the T4 genome. Positions of point mutations and deletions and percentages of recombination are indicated as in the legend to Fig. 6. The ends of gene e, 492 base pairs apart (18), are indicated by vertical dotted lines; the extents and positions of the deletions were determined by Wilson et al. (51). The line at the lower left indicates the scale of the figure. Crosses were performed in S/6/5 at 30°C (except under iii below) as described by Revel et al. (37). eG deletions and psu$_b$ strains were crossed to T4D$^+$ before use to remove an rIV ("spackle") mutation from the former and a gene 15 (amN133) mutation from the latter. eG deletions without rIV were recognized by their inability to plate on S/6/5 in the absence of added lysozyme, and psu$_b$ deletions without amN133 were recognized by their ability to plate on S/6/5 but not on CT439. The following conditions were used to score recombinants. (i) For crosses between goF3.03-2 and eG deletion mutants or amH26, progeny were plated (a) on S/6/5 plus lysozyme (500 μg/2 ml of top agar per plate) for total progeny and (b) on S/6/5 without lysozyme as a source of plaques for stabbing. Half as many plaques were found under plating condition (b) as under (a), as expected. To identify wild-type recombinants, plaques were stabbed onto HDF3.03 (nonpermissive) and S/6/5 (permissive). %R = WT × 100/plaques picked from S/6/5. (See legend to Fig. 6 for abbreviations.) (ii) For crosses between goF3.03-2 and psu$_b$ deletion mutants, progeny were plated on S/6/5 and stabbed onto HDF3.03 at 37°C, CT439 at 30°C, and S/6/5. Both recombinant classes were scored (on these indicators wild-type growth is zero, +, +, respectively; psu$_b$:goF growth is +, zero, +, respectively). %R = total recombinants × 100/plaques picked from S/6/5. The two recombinant classes were found in approximately equal numbers. (iii) The cross tsC3 × amH26 was performed in CR63 at 30°C; total progeny was determined on CR63 plus lysozyme at 30°C, and wild-type recombinants were determined on S/6/5 at 42°C. %R = WT × 200/total progeny. (iv) For tsC3 × eG223, progeny were plated on S/6/5 plus lysozyme at 30°C (total progeny) and S/6/5 at 37°C (wild-type recombinants). %R = WT × 200/total plaques. (v) For crosses of eG deletions with psu$_b$-Δ64, the total progeny was plated on S/6/5 plus lysozyme. Wild-type recombinants were scored by stabbing from S/6/5 (no lysozyme) onto CT439 at 30°C and S/6/5. %R = WT × 100/plaques picked from S/6/5. In all crosses, plaques were stabbed until at least 10 (and usually 20 to 40) recombinants had been identified. Where no recombinants are indicated, 500 (eG79 × goF3.03-2) or 3,791 (eG19 × goF3.03-2) plaques were tested.*

phenotype greatly retards growth of uninfected cells at 42°C. The active form of the host component must be present throughout T4 infection for production of phage.

Similarity of *hdf*, *hd*590, and *tabC* mutations. The mutant *E. coli* B strain HD590 (42) probably carries an *hdf* mutation, based on the close similarities of the HD590 and HDF phenotypes as reviewed in Results. The *tabC* mutations first described by Takahashi (43) also are probably allelic to *hdf* mutations. The two have similar map locations (5, 43; Stitt, in preparation), they cause similar defects in T4 infection, and strong compensatory T4 mutations (*comC*-α for *tabC*; *goF*1 for *hdf*) arise at very closely linked sites near T4 gene 39 (43, 44).

The significance of apparent differences between *tabC* and *hdf* mutants is difficult to judge because of the considerable allele-specific variations within each class. The *hdf*-0.26 phenotype is suppressed by *lon* (41), whereas the *tabC*^{cs}-110 and *C*-803 phenotypes are not (5). In *goF*1-infected *hdf* strains, certain early proteins still are underproduced or absent, whereas *comC*-α-infected *tabC* mutants show variable restoration of early functions depending on the *tabC* allele (5). Weakly compensating T4 mutations that grow on some of the host mutants are found near gene *e* for some *hdf* strains and in gene 45 for some *tabC* strains (43). Despite these variations, it seems likely that *hdf*, *hd*590, and *tabC* mutations occur in the same bacterial gene.

Are *hdf* mutations in *rho*? The pleiotropic nature of HDF phenotype suggests that the primary host defect may be in the control of protein synthesis. Possible defects could be in transcription initiation specificity, termination specificity, or translational factors. The following evidence suggests that *hdf* mutations lie in *rho*, the gene for transcription termination factor rho. Both *rho* (9, 16, 17) and *hdf* alleles (41; Stitt, in preparation) map at a similar site near *ilv* (83 min) in P1 transduction experiments. The *hdf*-0.26 mutation, like many *rho* defects, partially relieves the polarity of nonsense mutations (41). Genetic complementation tests with *rho*-15 (9) suggest that a *rho* defect blocks T4 growth in *tabC* hosts (5). Finally, lambda transducing phages that carry rho^+ lysogenize *hdf* strains, making them T4 sensitive (burst size, 100 at 37°C), whereas lambda phages carrying *rho-15* show much weaker complementation (burst size, 10) (Stitt, in preparation). These results must be interpreted with some caution, however, because *hdf*, *rho-15*, and the *tabC* mutants all were isolated after nitrosoguanidine mutagenesis, which tends to yield clustered multiple mutations (6, 14). Thus, it is possible that the complementation results are due to mutations at loci other than those of interest. The *hdf* defects themselves, however, probably represent single mutations in view of their frequency of occurrence and the frequent simultaneous reversion of HDF and *ts* phenotypes.

Are the observed *hdf* effects on T4 infection consistent with *hdf* mutations being in *rho*? Answering this question could help to clarify the presently unclear role of transcription termination in control of T4 gene expression.

Rho in T4 infection. In wild-type phage-infected cells, chloramphenicol inhibits the transcription of delayed early genes from immediate early promoters (13, 39), but in strong *rho* mutants like *rho-15* this inhibition is not seen (3). In vitro the action of *rho* has been shown to prevent delayed early transcription (19, 38, 46, 47). These results, and other less direct evidence that a T4 gene product is required for delayed early gene expression (26, 27), suggest that the phage produces a modulator of rho activity (antiterminator) early in infection. However, lack of rho activity also is deleterious; infection of strong *rho* temperature-sensitive mutants at nonpermissive temperature gives burst sizes 10- to 100-fold lower than does infection of wild-type cells (17; our unpublished data). Thus, the evidence so far suggests that both rho-mediated termination and modulation of rho by an early T4 gene product are required for normal transcription and production of phage progeny.

Early events in infection. The foregoing suggestion leads to the following specific model as one possible explanation for the effect of *hdf* mutations on early events in infection. HDF strains produce an altered rho, which at low temperature acts normally but at 37°C no longer can be modulated by the proposed early phage gene product that normally serves this function. As a result there is no synthesis of delayed early transcripts that depend upon read-through of termination signals after immediate early promoters. The *goF*1 mutations define the gene for the T4 termination modulator and alter it so that it can again modulate the altered rho, thereby overcoming the *hdf* block to infection. This model, similar to that proposed recently by Pulitzer and co-workers (5, 34) to explain the properties of *tabC* and *comC-α* mutations, is consistent with the observed effects of *hdf* and *goF*1 mutations. Pulitzer et al. (34), in addition, have reviewed the evidence that delayed early transcripts can arise either by read-through from adjacent immediate early genes or by initiation from a middle promoter under the positive control of the T4 *mot* gene (30), or both, and have shown strikingly that *mot*-defective phage infecting a *tabC* host make few if any delayed early gene products. These results support the dual mechanism for control of delayed early gene expression and the notion that *hdf* and *tabC* mutations alter rho so as to prevent its early modulation.

Late events in infection. In addition to aberrant early protein synthesis patterns, we have described specific deficiencies in late synthesis in HDF strains, leading to defects in assembly and retardation of the lysis mechanism. Some of these late effects could be secondary, resulting from alterations in DNA synthesis or gene expression earlier in infection. Alternatively, the immediate cessation of phage production after late temperature shift-up of $T4^+$-infected HDF cells suggests that Rho function is required throughout infection and raises the possibility that expression of some late genes may depend upon read-through of termination signals by the same modulated rho that is necessary for expression of delayed early genes.

Identity of the gene defined by *goF*1 mutations. Although *goF*1 and *comC-α* mutations have somewhat different effects in compensating for their respective host defects and map at nonidentical sites (cf. Fig. 4 and Fig. 1 of reference 44), they are within several hundred nucleotides of one another and therefore are likely to define the same gene, which has been proposed above to code for a modulator of rho. Based on map position, the *goF*1 mutations conceivably could be located in one of the two genes provisionally defined by *pla*CTr5x and *cef*

mutations, respectively. However, *del*(39-56)5, which covers *goF*1, plates on CTr5x(15), implying that the *goF*1 site is in a different gene than *pla*CTr5x. Similarly, the *cef* site is deleted in *del*(39-56)3 (15; A: Rodriguez-Prieto, Ph.D. thesis, Vanderbilt University, Nashville, Tenn., 1976) whereas *goF*1 is not (Fig. 6). Therefore, although the evidence is not conclusive, *goF*1 and *comC-α* probably define a new gene.

The putative modulator coded by this gene cannot be essential for normal T4 infection because *del*(39-56)12, which lacks the *goF*1 site, grows on wild-type hosts, although the burst size is only 60% that of normal (Rodriguez-Prieto, Ph.D. thesis). This result suggests that the *goF*1 gene product is a dispensable enhancer of T4 growth. Why the *hdf* defect should cause a lower progeny yield than do deletions of the *goF*1 site is not yet apparent. Perhaps *goF*1 function is dispensable only by virtue of the dual *rho/mot* control of most delayed early genes. The further work that will be necessary to understand this control should be aided by the availability of the *hdf* and *goF*1 mutants.

ACKNOWLEDGMENTS

These studies were supported by research grants to W.B.W. from the Public Health Service National Institute of Allergy and Infectious Diseases (AI-09238, AI-14994) and from the American Cancer Society, California Division (Special Grant 573). B.L.S. was also supported by a Public Health Service predoctoral training grant (GM-00086 from the National Institute of General Medical Science) to the California Institute of Technology, a Caltech Special Institute Fellowship, and the Arthur McCallum Fund.

LITERATURE CITED

1. **Benzer, S.** 1961. On the topography of the genetic fine structure. Proc. Natl. Acad. Sci. U.S.A. **47**:403-415.
2. **Blumenthal, T.** 1972. P1 transduction: formation of heterogenotes upon cotransduction of bacterial genes with a P2 prophage. Virology **47**:76-93.
3. **Brody, E., P. Daegelen, and D'Aubenton-Carafa.** 1978. The role of termination factor rho in the development of bacteriophage T4. Arch. Intern. Physiol. Biochim. **86**:897-898.
4. **Bujard, H., A. J. Mazaitio, and E. K. F. Bautz.** 1970. The size of the *r*II region of bacteriophage T4. Virology **42**:717-723.
5. **Caruso, M., A. Coppo, A. Manzi, and J. F. Pulitzer.** 1979. Host-virus interactions in the control of T4 prereplicative transcription. I. *tabC* (*rho*) mutants. J. Mol. Biol. **135**:959-977.
6. **Cerda-Olmedo, E., P. C. Hanawalt, and N. Guerola.** 1968. Mutagenesis of the replication point by nitrosoguanidine: map and pattern of replication of the *Escherichia coli* chromosome. J. Mol. Biol. **33**:705-719.
7. **Coppo, A., A. Manzi, J. F. Pulitzer, and H. Takahashi.** 1973. Abortive bacteriophage T4 head assembly in mutants of *Escherichia coli*. J. Mol. Biol. **76**:61-87.
8. **Cox, G. B., F. Gibson, and J. Pittard.** 1968. Mutant strains of *Escherichia coli* K-12 unable to form ubiquinone. J. Bacteriol. **95**:1591-1598.
9. **Das, A., D. Court, and S. Adhya.** 1976. Isolation and characterization of conditional lethal mutants of *Escherichia coli* defective in transcription termination factor *rho*. Proc. Natl. Acad. Sci. U.S.A. **73**:1959-1963.
10. **Edgar, R. S., R. P. Feyman, S. Klein, I. Lielausis, and C. M. Steinberg.** 1962. Mapping experiments with *r* mutants of bacteriophage T4D. Genetics **47**:179-186.
11. **Georgopoulos, C. P., R. W. Hendrix, A. D. Kaiser, and W. B. Wood.** 1972. Role of the host cell in bacteriophage morphogenesis: effects of a bacterial mutation on T4 head assembly. Nature (London) New Biol. **239**: 38-41.
12. **Goldfine, H.** 1969. Filter paper disk assay for lipid synthesis. Methods Enzymol. **14**:649-651.
13. **Grasso, R. J., and J. M. Buchanan.** 1969. Synthesis of early RNA in bacteriophage T4-infected *Escherichia coli* B. Nature (London) **224**:882-885.
14. **Guerola, N., J. L. Ingraham, and E. Cerda-Olmedo.** 1971. Induction of closely linked multiple mutations by nitrosoguanidine. Nature (London) New Biol. **230**:122-125.
15. **Homyk, T., Jr., and J. Weil.** 1974. Deletion analysis of two nonessential regions of the T4 genome. Virology 61: 505-523.
16. **Inoko, H., and M. Imai.** 1976. Isolation and genetic characterization of the *nitA* mutants of *Escherichia coli* affecting the termination factor rho. Mol. Gen. Genet. **143**:211-221.
17. **Inoko, H., K. Shigesada, and M. Imai.** 1977. Isolation and characterization of conditional-lethal rho mutants of *Escherichia coli*. Proc. Natl. Acad. Sci. U.S.A. **74**: 1162-1166.
18. **Inouye, M., M. Imada, and A. Tsugita.** 1970. The amino acid sequence of T4 phage lysozyme. IV. Dilute acid hydrolysis and the order of tryptic peptides. J. Biol. Chem. **245**:3479-3484.
19. **Jayaraman, R.** 1972. Transcription of bacteriophage T4 DNA by *Escherichia coli* RNA polymerase *in vitro*. Identification of some immediate-early and delayed-early genes. J. Mol. Biol. **70**:253-263.
20. **Kikuchi, Y., and J. King.** 1975. Genetic control of bacteriophage T4 baseplate morphogenesis. I. Sequential assembly of the major precursor, *in vivo* and *in vitro*. J. Mol. Biol. **99**:645-672.
21. **Kim, J.-S., and N. Davidson.** 1974. Electron microscope heteroduplex study of sequence relations of T2, T4 and T6 bacteriophage DNAs. Virology **57**:93-111.
22. **King, J.** 1968. Assembly of the tail of bacteriophage T4. J. Mol. Biol. **32**:231-262.
23. **Koplow, J., and H. Goldfine.** 1974. Alterations in the outer membrane of the cell envelope of heptose-deficient mutants of *Escherichia coli*. J. Bacteriol. **117**: 527-543.
24. **Kreuzer, K. N., K. McEntee, A. P. Geballe, and N. R. Cozzarelli.** 1978. Lambda transducing phages for the *nalA* gene of *Escherichia coli* and conditional lethal *nalA* mutations. Mol. Gen. Genet. **167**:129-137.
25. **Krisch, H. M., A. Bolle, and R. H. Epstein.** 1974. Regulation of the synthesis of bacteriophage T4 gene 32 protein. J. Mol. Biol. **88**:89-104.
26. **Linder, C. B., and O. Skold.** 1977. Evidence for a diffusible T4 bacteriophage protein governing the initiation of delayed early RNA synthesis. J. Virol. **21**:7-15.
27. **Linder, C. H., and O. Sköld.** 1980. Control of early gene expression of bacteriophage T4: involvement of the host *rho* factor and the *mot* gene of the bacteriophage. J. Virol. **33**:724-732.
28. **Low, B.** 1973. Rapid mapping of conditional and auxotrophic mutations in *Escherichia coli* K-12. J. Bacteriol. **113**:798-812.
29. **Mathews, C. K.** 1977. Reproduction of large virulent bacteriophages, p. 179-294. *In* H. Fraenkel-Conrat and R. R. Wagner (ed.) Comprehensive virology, vol. 7. Plenum Press, New York.
30. **Mattson, T., J. Richardson, and D. Goodin.** 1974.

Mutant of bacteriophage T4D affecting expression of many early genes. Nature (London) **250**:48–50.

31. **Mindich, L., J. Franzese-Sinclair, and J. Cohen.** 1976. The morphogenesis of bacteriophage ϕ6: particles formed by nonsense mutations. Virology **75**:224–231.
32. **Mufti, S., and H. Bernstein.** 1974. The DNA-delay mutants of bacteriophage T4. J. Virol. **14**:860–871.
33. **O'Farrell, P. Z., L. M. Gold, and W. M. Huang.** 1973. The identification of prereplicative bacteriophage T4 proteins. J. Biol. Chem. **248**:5499–5501.
34. **Pulitzer, J. F., A. Coppo, and M. Caruso.** 1979. Host-virus interactions in the control of T4 prereplicative transcription. II. Interaction between *tabC* (*rho*) mutants and T4 *mot* mutants. J. Mol. Biol. **135**:979–997.
35. **Pulitzer, J. F., and M. Yanagida.** 1971. Inactive T4 progeny virus formation in a temperature-sensitive mutant of *Escherichia coli* K12. Virology **45**:539–554.
36. **Radin, N. S.** 1969. Preparation of lipid extracts, Methods Enzymol. **14**:245–254.
37. **Revel, H. R., B. L. Stitt, I. Lielausis, and W. B. Wood.** 1980. Role of the host cell in bacteriophage T4 development. I. Characterization of host mutants that block T4 head assembly. J. Virol. **33**:366–376.
38. **Richardson, J. P.** 1970. Rho factor function in T4 RNA transcription. Cold Spring Harbor Symp. Quant. Biol. **35**:127–133.
39. **Salser, W., A. Bolle, and R. Epstein.** 1970. Transcription during bacteriophage T4 development: a demonstration that distinct subclasses of the "early" RNA appear at different times and that some are "turned off" at late times. J. Mol. Biol. **49**:271–295.
40. **Simon, L. D.** 1969. The infection of *Escherichia coli* by T2 and T4 bacteriophages as seen in the electron microscope. III. Membrane-associated intracellular bacteriophages. Virology **38**:285–296.
41. **Simon, L. D., M. Gottesman, K. Tomczak, and S. Gottesman.** 1979. Hyperdegradation of proteins in *Escherichia coli rho* mutants. Proc. Natl. Acad. Sci. U.S.A. **76**:1623–1627.
42. **Simon, L. D., D. Snover, and A. H. Doermann.** 1974. Bacterial mutation affecting T4 phage DNA synthesis and tail production. Nature (London) **252**:451–455.
43. **Takahashi, H.** 1978. Genetic and physiological characterization of *Escherichia coli* K12 mutants (*tabC*) which induce the abortive infection of bacteriophage T4. Virology **87**:256–265.
44. **Takahashi, H., and H. Yoshikawa.** 1979. Genetic study of a new early gene, *comC-α*, of bacteriophage T4. Virology **95**:215–217.
45. **Takano, T., and T. Kakefuda.** 1972. Involvement of a bacterial factor in morphogenesis of bacteriophage capsid. Nature (London) New Biol. **239**:34–38.
46. **Travers, A. A.** 1970. Positive control of transcription by a bacteriophage sigma factor. Nature (London) **225**: 1009–1012.
47. **Travers, A.** 1970. RNA polymerase and T4 development. Cold Spring Harbor Symp. Quant. Biol. **35**:241–251.
48. **Vanderslice, R. W., and C. D. Yegian.** 1974. The identification of late bacteriophage T4 proteins on sodium dodecyl sulfate polyacrylamide gels. Virology **60**:265–275.
49. **Ward, S., R. B. Luftig, J. H. Wilson, H. Eddleman, H. Lyle, and W. B. Wood.** 1970. Assembly of bacteriophage T4 tail fibers. II. Isolation and characterization of tail fiber precursors. J. Mol. Biol. **54**:15–31.
50. **Wilson, J. H.** 1973. Function of the bacteriophage T4 transfer RNAs. J. Mol. Biol. **74**:753–757.
51. **Wilson, J. H., J. S. Kim, and J. N. Abelson.** 1972. Bacteriophage T4 transfer RNA. III. Clustering of the genes for the T4 transfer RNAs. J. Mol. Biol. **71**:547–556.
52. **Wood, W. B., R. C. Dickson, R. J. Bishop, and H. R. Revel.** 1973. Self-assembly and non-self-assembly in bacteriophage T4 morphogenesis, p. 25–58. *In* R. Markham (ed.), The generation of subcellular structures, lst John Innes Symposium. North-Holland, Amsterdam.
53. **Wood, W. B., and H. R. Revel.** 1976. The genome of bacteriophage T4. Bacteriol. Rev. **40**:847–868.